Hindawi

Research Article

Cold Atmospheric Plasma Inhibits the Proliferation of CAL-62 Cells through the ROS-Mediated PI3K/Akt/mTOR Signaling Pathway

Fang Liu,[1,2] **Yuanyuan Zhou,**[1,2] **Wencheng Song** [iD][2,3] **and Hongzhi Wang** [iD][2,3]

[1]*Institutes of Physical Science and Information Technology, Anhui University, Hefei 230601, China*
[2]*Anhui Province Key Laboratory of Medical Physics and Technology, Institute of Health & Medical Technology,*
 Hefei Institutes of Physical Science, Chinese Academy of Sciences, Hefei 230031, China
[3]*Hefei Cancer Hospital, Chinese Academy of Sciences, Hefei 230031, China*

Correspondence should be addressed to Wencheng Song; wencsong@cmpt.ac.cn and Hongzhi Wang; wanghz@hfcas.ac.cn

This study aimed to investigate the inhibitory effects of cold atmospheric plasma (CAP) on anaplastic thyroid cancer cells (CAL-62 cells) and to reveal the molecular mechanism. The effects of CAP on CAL-62 cells were evaluated by cell viability, superoxide dismutase activity, apoptosis, cell cycle, and protein expression level, and the role of reactive oxygen species (ROS) produced by plasma was also investigated. The results showed that CAP dose-dependently inhibited cell viability and promotes cell apoptosis and G2/M arrest by increasing cell ROS levels. The activity of superoxide dismutase (SOD) was enhanced by CAP which indicated that the antioxidant system of the cell was activated. Additionally, the ROS produced by CAP can inhibit CAL-62 cell proliferation by inhibiting the PI3K/Akt/mTOR signaling pathway. Therefore, these findings will provide useful support for the application of CAP for treating anaplastic thyroid cancer.

1. Introduction

According to the most recent statistics from the American Cancer Society, the incidence and death rates of thyroid cancer in 2020 were 3.0% and 0.4%, respectively [1, 2]. Although anaplastic thyroid cancer (ATC) is one of the rarest types of thyroid cancer, it has a high mortality rate due to its easy metastasis and rapid development [3]. Traditional treatment methods including surgery, chemotherapy, and radiotherapy are the first choice for patients with ATC, but they cannot play an effective role in patients with advanced stages of ATC. When the cancer is confined to the gland and does not invade the capsule, radical thyroidectomy should be performed. However, only 10% of ATC patients can be radically resected, and most patients still cannot be completely resected. In addition, ATC is less sensitive to chemotherapy alone, and mostly elderly ATC patients with other underlying diseases often cannot tolerate the adverse reactions of chemotherapy drugs [4, 5]. Therefore, a new and effective treatment for ATC is urgently needed.

CAP is produced at a temperature close to room temperature, including UV, reactive species, electrons, and ions, which make it have a wider application prospect [6–8]. Studies have shown that CAP has a good effect on sterilization, wound healing, and oral therapy [9–11]. Since Fridman first reported that CAP promoted the apoptosis of melanoma cells in 2007, the antitumor effects of CAP have become a research hotspot in the field of plasma medicine [12]. Subsequently, the inhibitory effect of atmospheric plasma on lung cancer, cervical cancer, oral cancer, liver cancer, and melanoma cells has been gradually reported [13–17]. Extensive studies have shown that the concentration of active substances produced by CAP is closely related to its anticancer effects, especially H_2O_2, NO, and OH^- [18, 19]. Interestingly, studies have shown that the selectivity of anticancer effects of CAP is associated with increased

intracellular ROS levels induced by CAP [20]. CAP also plays an anticancer role by inducing DNA damage and promoting cell apoptosis, pyroptosis, and cell cycle arrest [21–25]. It has been reported that CAP treatment mainly induces oxidative stress to activate intracellular apoptosis pathways, such as P38/MAPK signaling pathway, ATM/P53 signaling pathway, and caspase cascade mitochondrial apoptotic pathway, which further leads to cell death [17, 26, 27]. The ROS produced by CAP plays an important role in inducing apoptosis. Current studies on the effect of CAP on thyroid cancer are limited; for example, Kim et al. reported that the intracellular ROS increase produced by plasma with He and O_2 as gas sources could not only induce the apoptosis of SW1763 cells by promoting the phosphorylation of JNK, P38, and caspase-3 but also inhibit the migration and invasion of thyroid papillary cancer cells [28, 29]. Apart from these two reports, CAP inhibition of thyroid cancer has rarely been reported. Recent studies have shown that CAP can inhibit the growth of 3D microtumor models and cancer cells in intestinal organoid models in vitro [30–32] and inhibit the growth of xenograft tumours in mice in vivo [33]. However, the mechanism of cancer cell death induced by CAP is still unclear.

In this study, CAP was applied to kill anaplastic thyroid cancer CAL-62 cells to explore its mechanism. The inhibitory effect of CAP on CAL-62 cells was studied by detecting cell viability, apoptosis, and cell cycle arrest, and changes in the levels of extracellular RONS and intracellular ROS were detected to study the effect of CAP treatment on intracellular and intracellular active substances. The effect of CAP on the antioxidant system of CAL-62 cells was also studied by SOD activity detection. In addition, the mechanism of CAP inhibition of CAL-62 cells was further studied through the PI3K/Akt/mTOR signaling pathway. This study will lay a theoretical basis for the clinical application of CAP for ATC.

2. Materials and Methods

2.1. Plasma Device and Cell Treatment. A schematic diagram of the CAP device is shown in Figure 1(a), and the CAP configuration that has been generated is shown in Figure 1(b). The dielectric barrier discharge (DBD) plasma device was used in this experiment. Four pairs of electrodes were evenly distributed in the reaction chamber, and a gas outlet was located on one side of the reaction chamber. The high-voltage electrode and ground electrodes were composed of round copper plates with diameters of 58 mm and 62 mm, respectively. The quartz medium (a thickness of 1 mm) was covered on the electrodes as a blocking medium. Helium (a purity of 99.999%) alone or helium plus oxygen, as the working gas in this experiment, entered the reaction chamber at a flow rate of 2.6 L/min. The cell culture dish (60 mm) with samples was placed on the grounding electrode, and the distance between the samples and quartz was controlled at 5 mm. Before each discharge, the working gas was delivered to the device for 90 seconds to remove the residual air in the device. The device operated at a power of 24.40 W and a frequency of 8.90 kHz which was measured using an oscilloscope (DSOX2024A, Sisha Rosa, USA) through the Lissajous method (Figure 1(c)).

2.2. Cell Culture. The human anaplastic thyroid cancer cell line CAL-62, human cervical cancer cell line HeLa, human brain glioma cell line (U118), human liver carcinoma cell line (HepG2), lung carcinoma cell line (A549), and human breast cancer cell line (MDA-MB-231) were purchased from Guangzhou Cellcook Biotech Co. All the cell lines were cultured in a DMEM medium (GIBCO, Carlsbad, CA, USA) containing 10% fetal bovine serum (LONSERA, Shanghai, China) and 1% penicillin-streptomycin (NCM Biotech, Suzhou, China) incubated at 37°C in an incubator containing 5% CO_2.

2.3. Cell Viability Assay. The MTT assay was used to determine the effects of CAP on cell viability. The cells were cultured in a 60 mm culture dish for 24 h after CAP treatment, the medium was discarded, and then, a 1 ml cell medium containing 10% MTT (Sigma-Aldrich, USA) solution was added and incubated at 37°C for 4 h. The supernatant was discarded, 2 ml dimethyl sulfoxide (DMSO, Sangon Biotech, Shanghai, China) was added to the culture dish, and then, the suspension was fully dissolved and mixed. Finally, the absorbance at 492 nm was determined using an enzyme plate analyzer (Hiwell-Diatek, Wuxi, China).

2.4. ROS Detection. High electron density was generated during discharge in a DBD plasma device, and the cell culture medium provided a sufficient liquid environment. Under these conditions, water vapour gains electrons to produce H_2O_2. When the plasma interacted with the liquid surface, the water molecules can capture the excited state of the material, further producing active substances (such as H_2O_2, and NO) in the liquid phase [34]. Therefore, the H_2O_2 content was present in the cell culture medium after CAP treatment. The H_2O_2 level in the CAP-treated cell culture medium was determined using a hydrogen peroxide assay kit (Beyotime Biotechnology, Shanghai, China). After CAP treatment (0 s, 5 s, 10 s, 15 s, 20 s, and 30 s), 50 μl medium was immediately added to the 96-well plate, and then a 100 μl hydrogen peroxide detection reagent was added according to kit instructions. The absorbance at 560 nm was determined using an enzyme plate analyzer.

The intracellular ROS levels were detected by a fluorescent probe DCFH-DA (Beyotime Biotechnology, Shanghai, China). After CAP treatment (0 s, 15 s, 30 s) or 5 mM ROS scavengers (N-acetyl-l-cysteine, NAC) treatment for 2 h, the culture was incubated at 37°C for 6 h, the original medium was discarded, washed with PBS, and then, DCFH-DA (2 μM) at 37°C was added and incubated for 30 min in the dark. The supernatant was discarded and cleaned with phosphate-buffered saline (PBS) 3 times. Finally, the fluorescence intensity was observed using a fluorescence microscope (Olympus, Tokyo, Japan).

2.5. Detection of SOD Activity. The activity of SOD was detected using a superoxide dismutase activity detection kit (Sangon Biotech, Shanghai, China). After CAP treatment (0 s, 15 s, 30 s, and 30 s + NAC) for 24 h culture, cells were
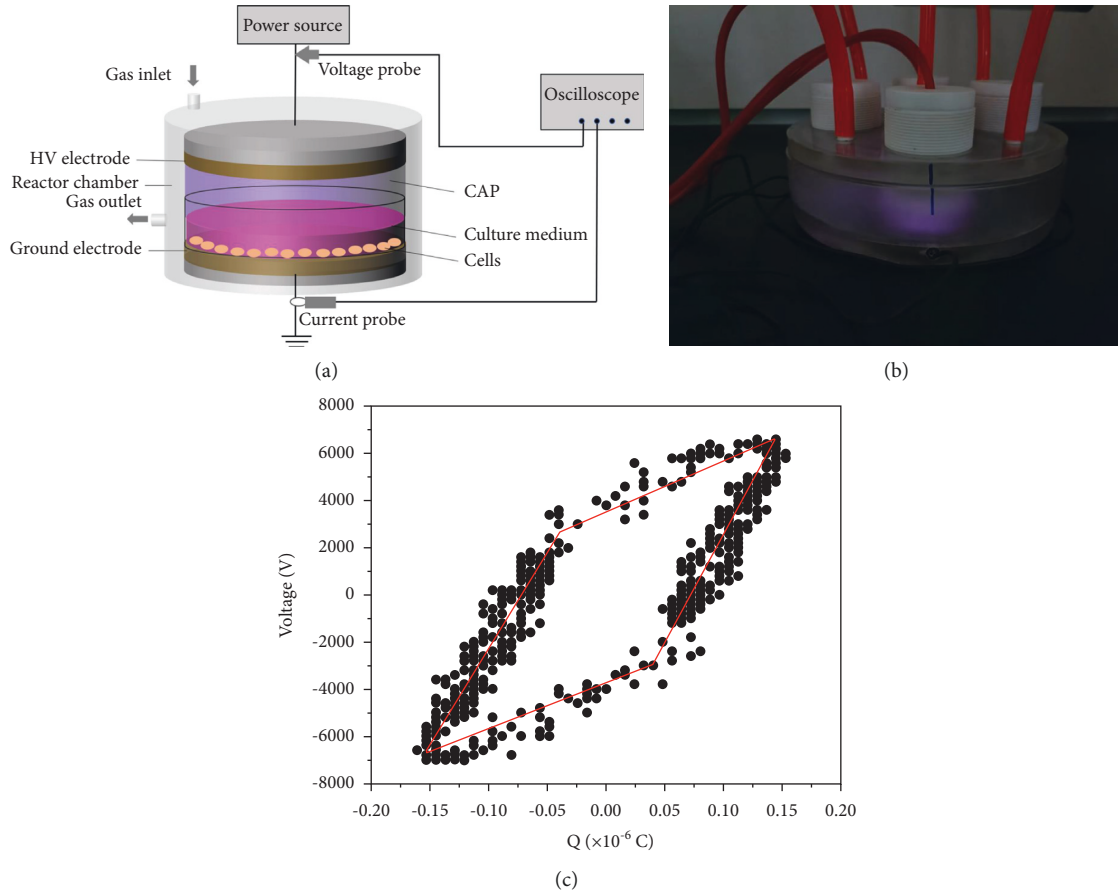
FIGURE 1: (a) Schematic diagram of the atmospheric pressure DBD plasma device. (b) Image of CAP that has been generated. (c) The V-Q Lissajous pattern of DBD.

collected in a centrifuge tube. Following the manufacturer's instructions, the absorbance at 560 nm was determined using an enzyme plate analyzer (Hiwell-Diatek, WuXi, China).

2.6. NO Detection. The NO level in the plasma-treated cell culture medium was determined using a nitric oxide assay kit (Beyotime Biotechnology, Shanghai, China). After CAP treatment (0 s, 5 s, 10 s, 15 s, 20 s, and 30 s), 50 μl of the medium was immediately added to the 96-well plate, then 50 μl Griess Reagent I and 50 μl Griess Reagent II were added in turn according to kit instructions. The absorbance at 560 nm was determined using an enzyme plate analyzer (Hiwell-Diatek, WuXi, China).

2.7. Apoptosis Detection. Cell apoptosis was detected using an annexin V-FITC apoptosis detection kit (Beyotime Biotechnology, Shanghai, China). After CAP treatment (0 s, 15 s, 30 s, and 30 s + NAC) for 24 h culture, the medium was discarded, and the cells were washed with PBS three times. Subsequently, the cells were digested with trypsin without EDTA, collected by centrifugation, and washed 3 times with PBS. The binding buffer, annexin V-FITC, and propidium

iodide were added in turn. Finally, the samples were examined by flow cytometry.

2.8. Cell Cycle Analysis. The cell cycle was detected using the cell cycle analysis kit (Beyotime Biotechnology, Shanghai, China). After CAP treatment (0 s, 5 s, 10 s, 15 s, and 30 s + NAC) for 24 h culture, the medium was discarded, and the cells were washed three times with PBS. Subsequently, the cells were digested with trypsin, collected by centrifugation, and fixed in 70% ice-cold ethanol for 12 h. The binding buffer, RNase A, and Propidium Iodide were added in turn. Finally, the samples were examined by flow cytometry.

2.9. Western Blot. CAL-62 cells were exposed to CAP for 0 s, 15 s, and 30 s with or without NAC. Ice-cold PBS was used to clean cells, and RIPA was used to lysate cells. Samples were placed on ice and lysed for 30 min. Subsequently, samples were collected in a 1.5 ml centrifuge tube, ice lysed for 20 min, and oscillated every five minutes. The obtained samples were further centrifuged at 10000g for 30 min, and then, the centrifuged supernatants were collected and heated at 100°C for 10 min. SDS-PAGE (sodium dodecyl sulfate-polyacrylamide gel electrophoresis) was performed using

10% PAGE gels. Proteins were transferred to the NC membrane and then incubated with 5% skim milk for 1 h and washed with TBST. The membrane was incubated overnight with a specific antibody diluent at 4°C and washed with TBST 3 times for 10 min. Subsequently, the membrane was incubated with horseradish peroxidase-coupled secondary antibodies for 1 h at room temperature. In the end, the membrane was washed with TBST 3 times for 10 min and visualized by chemiluminescence.

2.10. Statistical Analysis. Statistical analysis was performed on data obtained from at least three independent experiments, and the data were expressed as standard deviation. The significance level was assessed by one-way analysis of variance (ANOVA). *p* value <0.05 between two independent groups was considered a statistically significant difference.

3. Results and Discussion

3.1. CAP Inhibited the Cell Viability of Cancer Cells. The effect of CAP on the cell viability was evaluated after the cells were treated with CAP for 10 s, 20 s, 30 s, and 40 s. The cell viability of all types of cancer cells in this study (CAL-62, MDA-MB-321, HeLa, U118, HepG2, and A549 cell lines) decreased in a time-dependent manner (Figure 2(a)). The sensitivity of different cell lines can be compared under the same conditions, and CAL-62 cells were the most sensitive cell lines. After plasma treatment for 10 s, the cell viability of CAL-62 cells decreased significantly and dropped to less than 50% after 20 s treatment. Then, the viability of CAL-62 cells was detected by further refining the treatment time (Figure 2(b)). Interestingly, when the CAP treatment time exceeded 15 s, the cell viability reduced significantly. The cell viability decreased to 99.86 ± 3.33, 92.30 ± 3.32, 57.60 ± 2.33, 46.17 ± 3.20, and $39.16 \pm 2.94\%$ of the control after plasma treatment for 5 s, 10 s, 15 s, 20 s, and 30 s, respectively. To test the effects of different gas treatments on CAL-62 cells, we treated the cells with helium, argon, and air for 15 s, and then, the changes in cell viability were measured. The results showed that the effect of helium discharge was better than that of argon and air discharge (Figure 2(c)). Subsequently, CAL-62 cell viability under different helium and oxygen ratios was measured (Figure 2(d)). When helium is filled with 5% oxygen, the cell viability decreased to 97.57 ± 3.95, 96.29 ± 2.93, 81.50 ± 1.09, 65.11 ± 0.47, and $36.64 \pm 0.84\%$ of the control after plasma treatment for 5 s, 10 s, 15 s, 20 s, and 30 s, respectively. When helium is filled with 10% oxygen, the cell viability decreased to 98.57 ± 3.01, 98.20 ± 4.49, 75.56 ± 0.09, 68.95 ± 0.61, and $29.65 \pm 0.27\%$ of the control after plasma treatment for 5 s, 10 s, 15 s, 20 s, and 30 s, respectively. The experimental results showed that among the three gas modes, CAP with pure helium as the working gas had a better inhibitory effect on cell viability.

The sensitivity of cancer cells to CAP varied by different cell lines [35], and CAL-62 showed the best sensitivity among several cancer cells used in this study. Some scholars believed that the different cell culture medium types of cells were mainly related to the sensitivity of different cell lines to

plasma, and different components in the cell culture medium interacted with CAP to produce the killing effects [36, 37]. A lack of pyruvate in a plasma-activated medium increases the damage to cancer or normal cells and reduces the selectivity of plasma [38]. However, the effect of this condition can be eliminated using the DMEM medium for all cell lines used in this experiment. The different sensitivities were probably determined by cell type and were related to the properties of the cells themselves.

There are three hypotheses to explain the sensitivity of plasma-treated cancer cells, all of which focus on cell membranes. The first view is that the content of aquaporin on the cell surface is the key to the sensitivity of the cell to plasma [25]. Aquaporin allows ROS to enter the cell and cause cell damage. The second view is that redox-related enzymes (such as catalase, NADPH oxidases, myeloperoxidase, and nitric oxide synthases) on the cell membrane can amplify the ROS produced by plasma; therefore, the content of redox-related enzymes on the cell membrane is an important reason for the sensitivity of cells to plasma [39]. The last idea is that lower cholesterol levels increase membrane oxidation and void formation, and cells show higher sensitivity to plasma [40]. Sander et al. further analyzed three hypotheses on the causes of plasma sensitivity of 38 human cell lines by studying 33 surface molecules [41]. The results showed that the expression levels of aquaporin and redox-related enzymes failed to explain the plasma-induced sensitivity. However, the cholesterol content of the cell membrane was positively correlated with the plasma treatment resistance. On this basis, they also found a high correlation between cell metabolism and plasma-induced cytotoxicity. In summary, the difference in the performance of different cells with plasma treatment is due to the difference in the amount of ROS entering the cell and the different responses of the cell to the ROS signal. The cells used in our experiments, such as A549, HeLa, HepG2, and U118, belong to the 38 cell lines studied by Sander et al. In addition to the aforementioned factors, the influence of aquaporin activity and redox-enzyme activity should be considered.

3.2. CAP Increased Extracellular ROS and RNS Levels. The contents of H_2O_2 and NO in the culture medium were determined immediately after CAP treatment. As shown in Figure 3, the reactive oxygen and nitrogen species (RONS) increased as the CAP processing time increased. After CAP treatment for 0 s, 5 s, 10 s, 15 s, 20 s, and 30 s with pure helium as the working gas, the concentration of H_2O_2 was 0.29 ± 0.04, 2.88 ± 0.24, 13.96 ± 0.24, 43.81 ± 0.46, 43.61 ± 0.46, and $43.16 \pm 0.82\,\mu\text{Mol/L}$ (Figure 3(a)), respectively. When helium was filled with 5% oxygen, the concentration of H_2O_2 was 0.23 ± 0.48, 1.67 ± 0.32, 8.86 ± 1.37, 29.09 ± 2.35, 44.29 ± 0.32, and $44.91 \pm 0.91\,\mu\text{Mol/L}$, respectively. When helium was filled with 10% oxygen, the concentration of H_2O_2 was 0.73 ± 0.58, 1.061 ± 0.31, 19.99 ± 3.51, 39.46 ± 1.58, 42.05 ± 3.26, and $44.38 \pm 0.98\,\mu\text{Mol/L}$, respectively. Adding oxygen to the working gas did not produce more H_2O_2 in the cell culture medium. Besides, the concentration of NO was 10.58 ± 7.64, 24.75 ± 2.50, 28.08 ± 2.89, 42.25 ± 10.00, 48.08 ± 16.65, and $75.58 \pm 3.82\,\mu\text{Mol/L}$, respectively (Figure 3(b)).
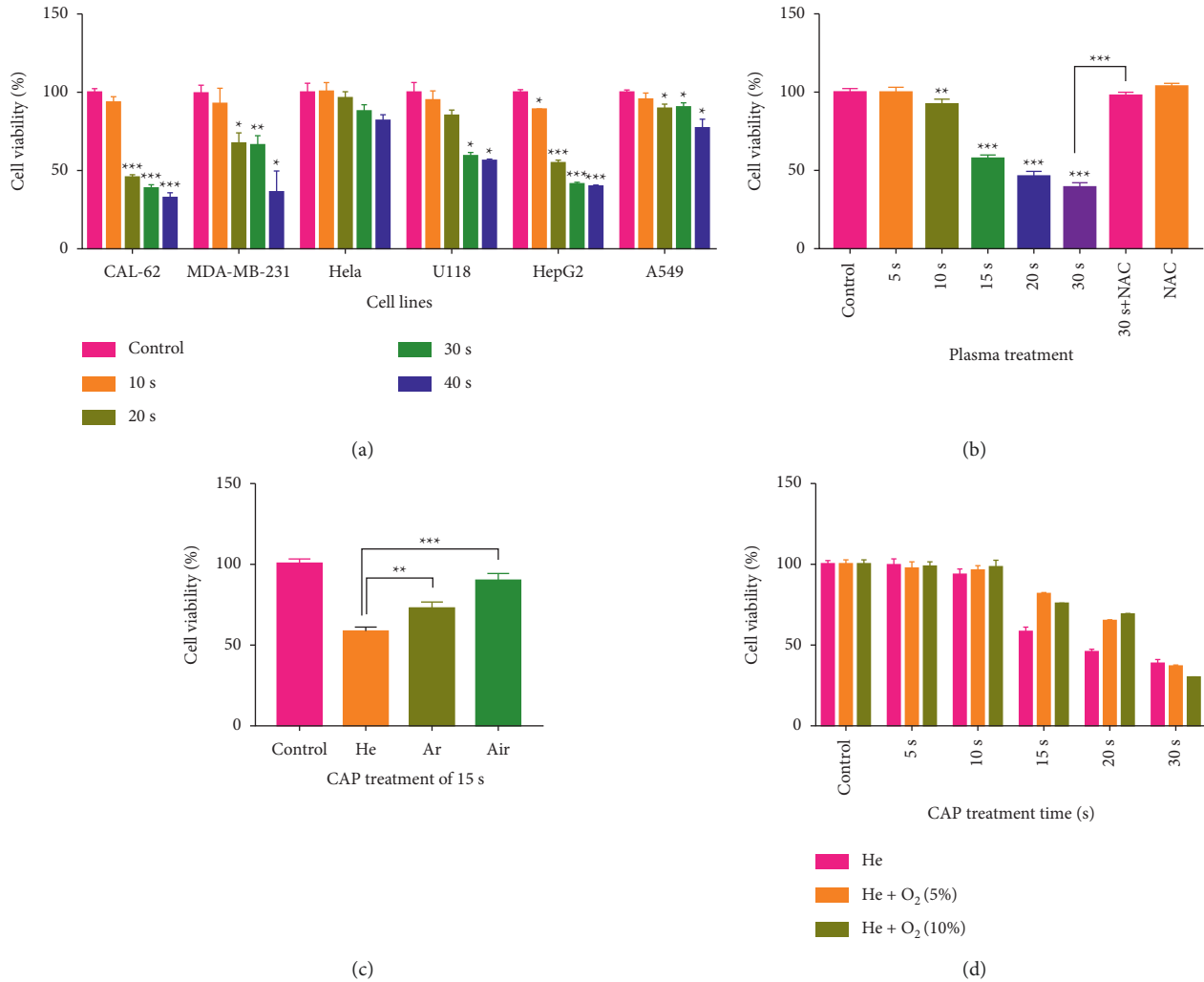
(a)

(b)

(c)

(d)

FIGURE 2: Cell viability assay on cancer cells. (a) CAL-62, MDA-MB-231, HeLa, U118, HepG2, and A549 cells treated with CAP for 10 s, 20 s, 30 s, and 40 s, or without CAP treatment. (b) The effect of NAC on the viability of CAL-62 cells. (c) CAL-62 cells treated with the gas of helium, argon, and air for 15 s. (d) CAL-62 cells treated with CAP for 0 s, 5 s, 10 s, 15 s, 20 s, and 30 s, and CAP treated in the different oxygen ratios of working gases. At 24 hours after plasma treatment, cell viability was measured by the MTT assay. Data represent the mean ± SD of three independent experiments. $^{*}p < 0.05$, $^{**}p < 0.01$, and $^{***}p < 0.001$ with ANOVA compared with the control.

There are many kinds of CAP generating devices, but they can be divided into two categories according to the discharging principle: plasma jet and DBD [42, 43]. The continuous improvement and development of CAP devices provide the basis for developing CAP in the biomedical field [44–46], a DBD device was used in our experiment. As a part of the cathode, the sample to be treated could generate a stable large area of plasma beam, and the CAP first touched the medium [47–49]. The active substance produced by the CAP plays a critical role in anticancer [50]. Studies have shown that H_2O_2, NO_2^-, $ONOO^-$, and other active substances can be widely detected in the plasma-activated medium [51].

3.3. Intracellular Reactive ROS and SOD Activity Increased after CAP Treatment. As shown in Figure 4, fluorescence intensity represented intracellular ROS intensity, and the

intracellular ROS increased in a time-dependent manner. The fluorescence was the brightest after 30 s of CAP treatment, representing the highest intracellular ROS. Additionally, NAC pretreated cells showed no significant increase in ROS even after 30 s of plasma treatment (Figure 4(a)). The results of this experiment showed a trend consistent with the results of the cell viability experiment with no significant change from 0 s to 15 s. The decrease of cell viability after 30 s of treatment was correlated with the increase of intracellular ROS. It was reported that ROS plays a critical role in cell response to the plasma treatment [22, 52]. It was found that plasma can selectively promote the ROS levels in cancer cells, and A549 cells can produce more ROS than BEAS-2B cells under the same dose of plasma treatment [53]. SOD is the main producing enzyme of hydrogen peroxide and plays an important role in biological antioxidant systems [54]. Changes in SOD activity in cells were detected after

CAP treatment, and the results are shown in Figure 4(c). CAP treatment can increase the activity of SOD in cells, indicating that CAP treatment can activate the antioxidant system in cells to a certain extent.

3.4. CAP Induced Apoptosis and Cell Cycle Arrest in CAL-62 Cells.
To further explore the effect of CAP on apoptosis, a FITC-annexin V/PI double staining experiment was conducted. All cells were divided into the following groups; Annexin V−/PI− (the lower left quadrant), Annexin V−/PI+ (the upper left quadrant), Annexin V+/PI+ (the upper right quadrant), and Annexin V+/PI− (the lower right quadrant). Cells in the parts of Annexin V−/PI− and Annexin V−/PI+ represented liver and necrosis cells, respectively. The apoptotic cells were composed of Annexin V+/PI− and Annexin V+/PI+ parts, which represented early apoptosis and late apoptosis cells, respectively. The results showed that CAP treatment for a certain period could increase the apoptosis of CAL-62 cells (Figure 5). Although the MTT results showed that 15 s of treatment could significantly inhibit cell viability (Figure 2(b)), the promotion of cell apoptosis was not significant with 8.98% apoptosis (Figure 5(B)). However, the apoptosis rate of cells with 30 s of plasma treatment can reach 84.38% (Figure 5(C)). Additionally, the addition of NAC resisted the damage effects of CAP on cells and reduced cell apoptosis (Figure 5(D)). Apoptosis is an important pathway in CAP-induced cell death. Studies have shown that CAP treatment can induce tumor cell apoptosis to varying degrees, thus exerting its anticancer effect [22, 26, 53]. In addition, compared with traditional chemotherapy and radiotherapy, CAP showed a better apoptotic effect on ATC cells. A report of ATC cells treated with apatinib showed that the apoptosis rate of cells was only 23.74% even under apatinib treatment of 40 μM [55]. When the intensity of X-ray treatment was 6 Gy, the apoptosis of ATC cells was still feeble, only about 10%, even after incubation for 50 h [56].

Moreover, CAP dose-dependently induced apoptosis [57, 58], which was consistent with our research results. Interestingly, cell viability was significantly decreased in the 15 s CAP-treatment group compared with the control group, while apoptosis was not evident. We speculated that this might be due to the small dose of CAP during the 15 s treatment, which inhibited cell proliferation but was not enough to induce cell apoptosis. To assess the effect of CAP on the cell cycle, flow cytometry was used to detect different cell cycle contents. The G2/M phase of CAL-62 cells increased after CAP treatment (Figure 6), and the G2/M phase arrest of cells might be due to DNA damage, initiating cell cycle checkpoints to block mitotic processes [19]. CAP produces RONS that induce DNA damage leading to cell cycle arrest and apoptosis [59]. In our experiment, the addition of NAC can significantly offset the G2/M arrest caused by CAP, indicating that ROS plays an important role (Figure 6(f)).

3.5. Protein Expression Level Changed after CAP Treatment.
In the aforementioned studies, the inhibitory effect of CAP treatment on CAL-62 cell proliferation had been studied.

Subsequently, the specific mechanism of CAP's inhibitory effect on cancer was further explored, and the expression of PI3K, Akt, and mTOR was detected. The western blotting results showed that the expression levels of PI3K, Akt, and mTOR dose-dependently decreased with the CAP treatment time increase (Figure 7). Additionally, the expression of VEGF, Ras, and ERK1/2 also dose-dependently decreased with the CAP treatment time increase.

There have been many studies on the anticancer effects of CAP. However, the specific molecular mechanism of anticancer effects of CAP is not very clear. We found that CAP could inhibit the proliferation of CAL-62 cells by inhibiting the PI3K/Akt/mTOR signaling pathway (Figure 8). As a key pathway of cell proliferation, the PI3K/Akt/mTOR signaling pathway is often overexpressed in tumour cells, and the inhibition of this pathway can achieve the effect of inhibiting tumour growth [60]. Studies have shown that PI3K/Akt inactivation can inactivate mTOR, thereby inhibiting cell proliferation and promoting cell apoptosis [61–63]. Studies have also shown that ROS plays an important role in the inactivation of this pathway. Silica nanoparticles can mediate the inactivation of the PI3K/Akt/mTOR signaling pathway through ROS, and then trigger the apoptosis and autophagy of vascular endothelial cells [64]. In this study, the intracellular ROS level time-dependently increased with CAP treatment while the protein expression of PI3K, Akt, and mTOR time-dependently decreased. Besides, the addition of NAC could significantly increase the protein expressions of PI3K, Akt, and mTOR, which also indicated that ROS can mediate this pathway.

3.6. Effect of NAC on CAP Treatment.
To further observe the role of ROS in CAP-treated CAL-62 cells, NAC was used to remove ROS from the treated samples. After NAC pretreatment, the cell viability did not decrease significantly even after 30 s of CAP treatment (Figure 2(b)). To verify the scavenging effect of NAC on intracellular ROS, intracellular ROS after combined treatment with NAC and CAP was detected, and the results showed that there was no significant difference in ROS levels between the control group and the NAC group (Figure 4). In addition, the combined treatment of NAC and CAP can effectively reduce the rate of apoptotic cells and resist the inhibitory effect of CAP on the PI3K/Akt/mTOR signaling pathway (Figure 7). These results indicated that the addition of NAC effectively removed ROS in the treated cells, and ROS played an important role in the effect of CAP on CAL-62 cells.

As for the killing mechanism of CAP on cancer cells, a view is that active substances such as RONS produced by CAP play a decisive role, which can cause DNA damage and induce oxidation. RONS are classified into short-lived and long-lived substances, and long-lived substances, such as hydrogen peroxide, nitrite, and nitrate, play a critical role in the anticancer effects of CAP [65]. In this study, NAC was used to explore the role of ROS in CAP-killing CAL-62 cells. Interestingly, NAC can largely offset the cell damage caused by CAP. Ma et al. elaborated on the contribution of hydrogen peroxide to CAP damage cells, which was consistent
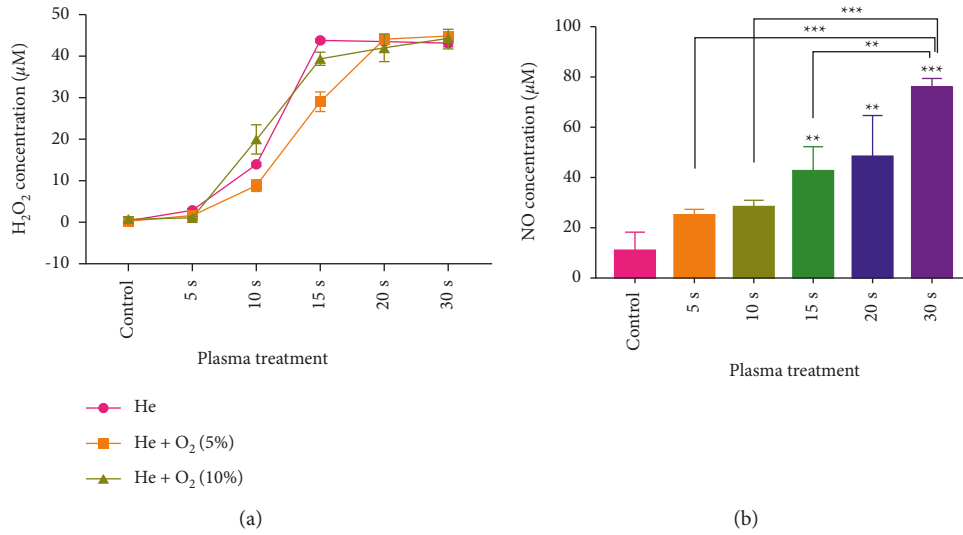
(a)

(b)

FIGURE 3: Extracellular H_2O_2 and NO content. (a) The concentrations of H_2O_2 in the cell culture medium after CAP treatment for 0 s, 5 s, 10 s, 15 s, 20 s, and 30 s. (b) The concentrations of NO in the cell culture medium after CAP treatment for 0 s, 5 s, 10 s, 15 s, 20 s, and 30 s. Data represent the mean $\pm$ SD of three independent experiments. $^*p < 0.05$, $^{**}p < 0.01$, and $^{***}p < 0.001$ with ANOVA compared with the control.
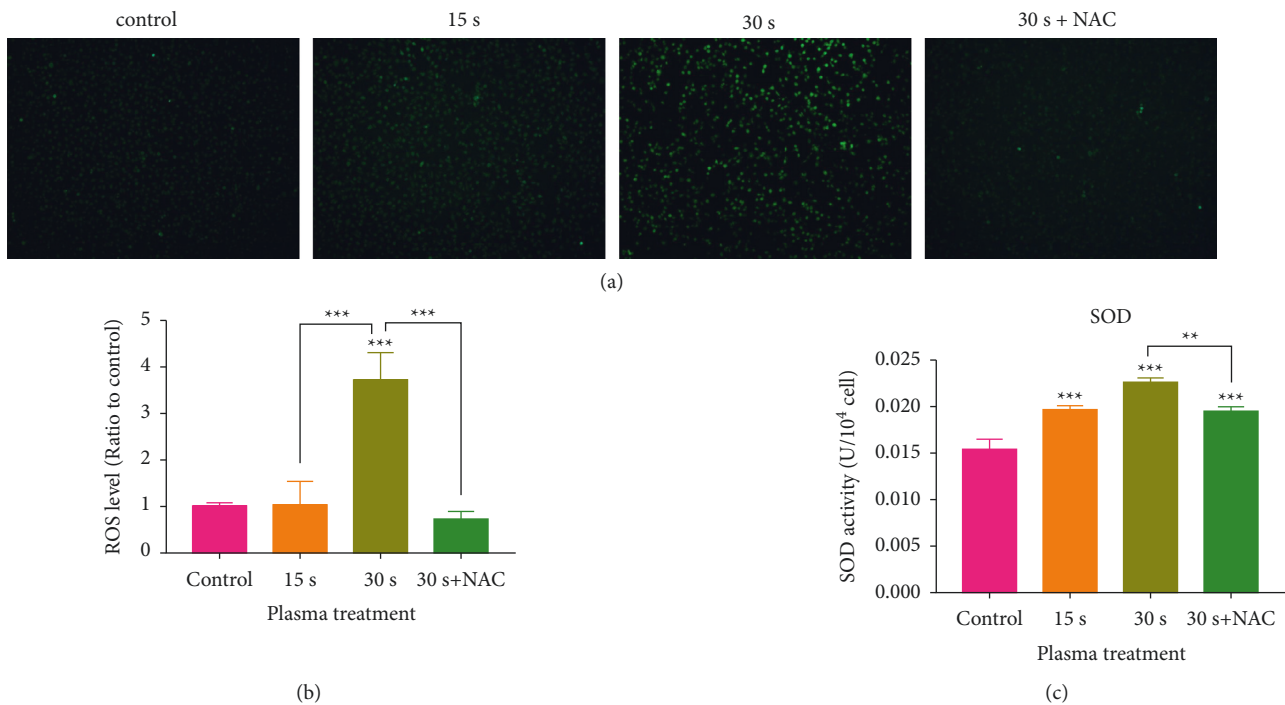

(a)

(b)

(c)

FIGURE 4: Intracellular ROS levels. (a) Fluorescence images of intracellular ROS generation in CAL-62 cells. (b) The quantification by measuring fluorescence pixel intensity using ImageJ software. (c) The activity of SOD in CAL-62 cells. The data represent the mean $\pm$ SD of three independent experiments. $^*p < 0.05$, $^{**}p < 0.01$, and $^{***}p < 0.001$ with ANOVA compared with the control.

with our experimental results [18]. A molecular dynamic simulation showed that ROS in CAP can damage DNA at the atomic level, breaking important chemical bonds in DNA and the genes of cancer cells [66]. However, the role of RNS in CAP-killing cancer cells should not be ignored, and the important role of NO was demonstrated. Increasing the

supply of nitrite and nitrate can improve the yield of ONOO- after CAP treatment and play an anticancer effect [67]. NO free radical produced by CAP can cause EGFR degradation and dysfunction in oral squamous cell carcinomas overexpressed with an epidermal growth factor, further resulting in cell damage [68]. A recent study showed that hydrogen
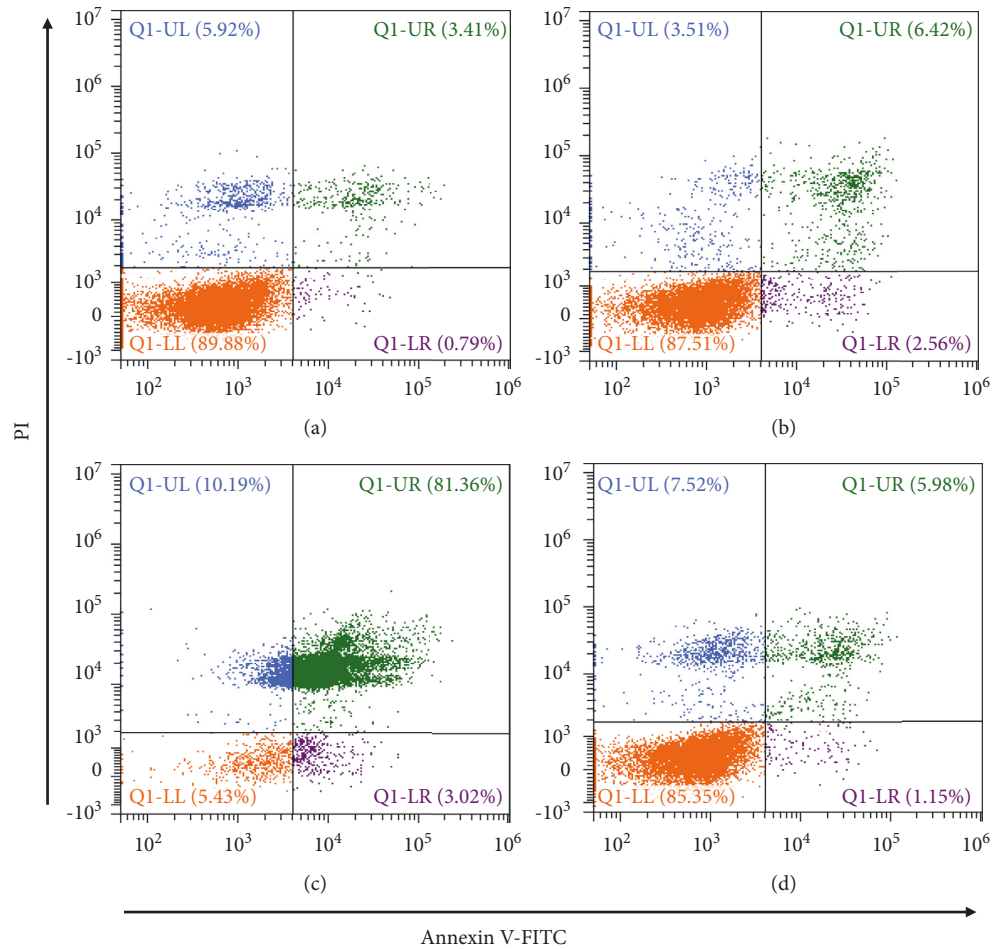
Figure 5: CAP-induced apoptosis rates of CAL-62 cells in (a) control, (b) 15 s CAP-treated cells, (c) 30 s CAP-treated cells, and (d) 30 s CAP- and NAC-treated cells. In each small image, the lower left quadrant represents living cells, while the lower right quadrant and the upper right quadrant represent early and late apoptotic cells, respectively.
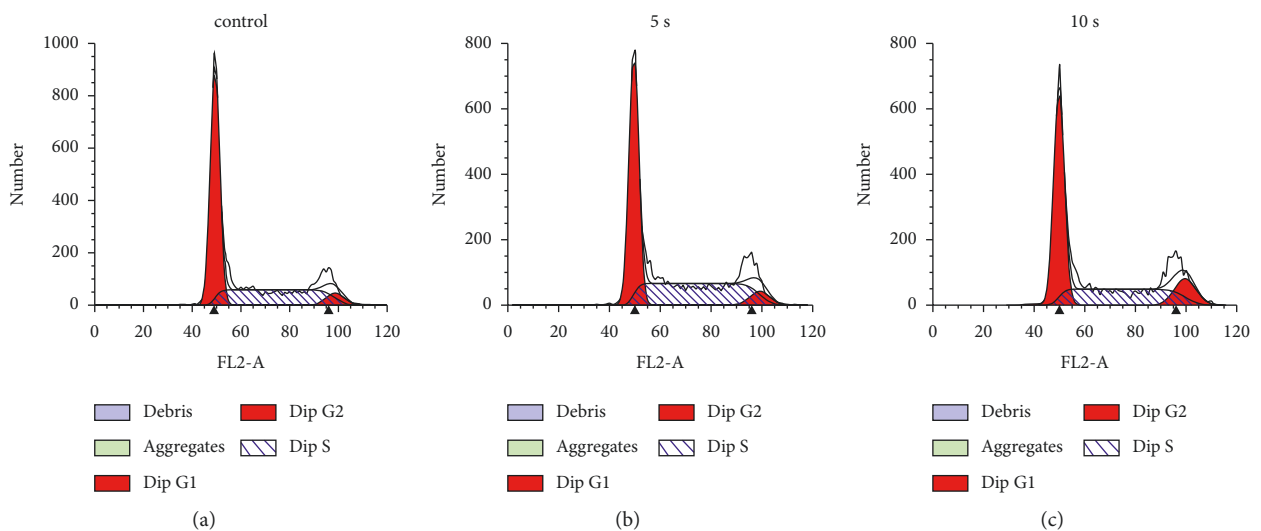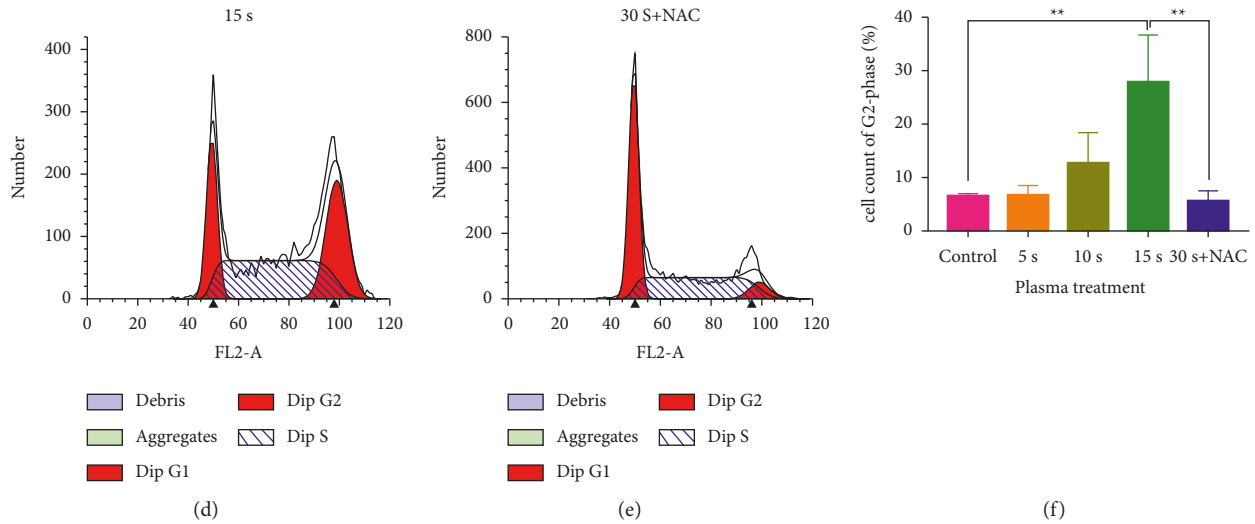

Figure 6: Continued.

(d)

(e)

(f)

Figure 6: CAP-induced cell cycle arrest of CAL-62 cells in (a) control, (b) 5 s CAP-treated cells, (c) 10 s CAP-treated cells, (d) 15 s CAP-treated cells, and (e) 30 s CAP and NAC-treated cells. (f) Cell population in the G2 phase is represented as a percentage of the total cells. Data represent the mean ± SD of three independent experiments. $^*p < 0.05$, $^{**}p < 0.01$, and $^{***}p < 0.001$ with ANOVA compared with the control.
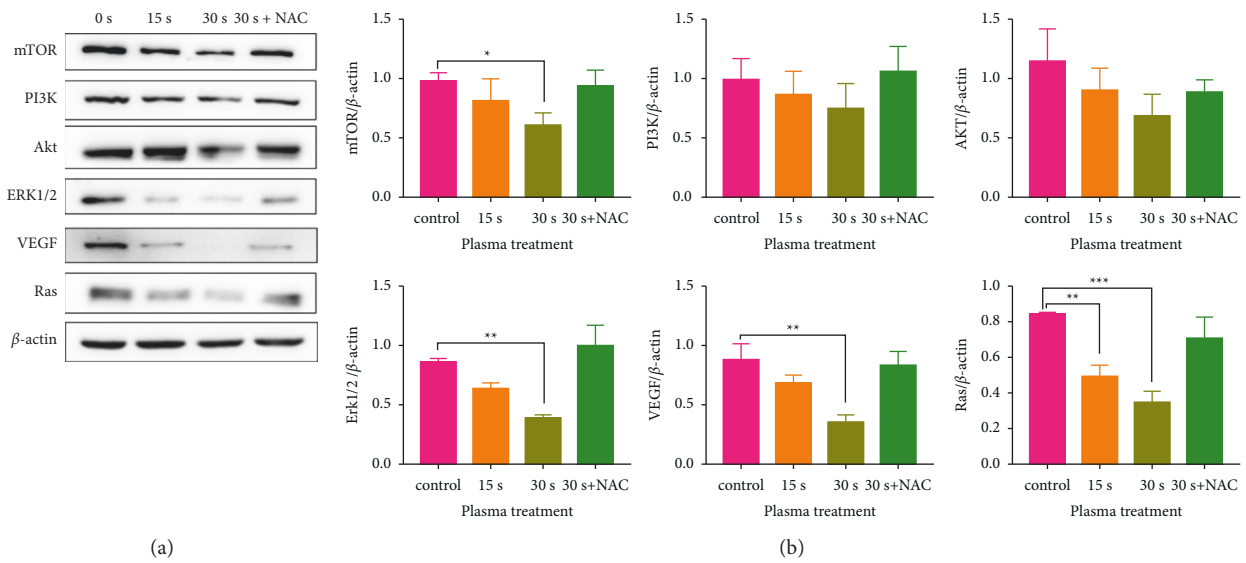

(a)

(b)

Figure 7: CAP treatment-induced changes in protein expression levels. (a) CAP affected the expression of PI3K, Akt, mTOR, Erk1/2, VEGF, and Ras. (b) The quantification by measuring the protein expression with ImageJ software.
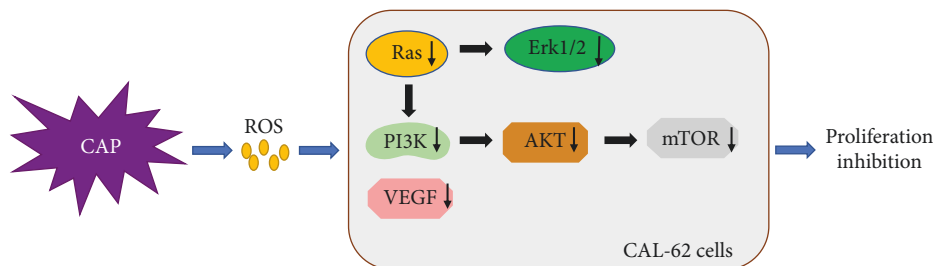

Figure 8: A schematic representation of the mechanism of CAP inhibits the proliferation of CAL-62. ROS produced by CAP can inhibit the expression of PI3K, Akt, mTOR, Ras, Erk1/2, and VEGF.

peroxide and nitrite directly work together to activate the mitochondrial apoptotic pathway of cells and induce cell death [69]. Of course, this study is just preliminary research on the inhibitory effect of CAP on CAL-62 cells. The selective effect of CAP on different types of cancer cells is also reflected in our experimental results. Exploring why CAP selectively kills cancer cells is an important part of future work. In addition, animal and clinical trials are needed in the future. However, the regulation of intracellular signaling pathways by CAP is a very complex process involving multiple pathways, and it is still a challenge to elucidate the mechanism of CAP against cancer cells.

4. Conclusion

In this study, the anticancer effect of undifferentiated thyroid carcinoma CAL-62 cells by CAP was reported for the first time. CAP treatment dose-dependently increased the level of ROS, and the expression of PI3K, Akt, mTOR, Ras, and Erk1/2 decreased with the increase of the CAP treatment dose. CAP could significantly inhibit the cell viability of CAL-62 cells and induce apoptosis and G2/M arrest. However, the addition of NAC largely decreased the effect of CAP on CAL-62 cells. These results suggest that ROS produced by CAP can inhibit CAL-62 cell proliferation by inhibiting the signaling pathway. Therefore, these findings will provide useful support for the application of CAP for treating undifferentiated thyroid cancer.

Data Availability

The data that support the findings of this study are available from the corresponding author upon reasonable request.

Conflicts of Interest

The authors declare that they have no conflicts of interest.

Acknowledgments

References

[1] H. Sung, J. Ferlay, R. L. Siegel et al., "Global cancer statistics 2020: GLOBOCAN estimates of incidence and mortality worldwide for 36 cancers in 185 countries," *CA-Cancer Journal for Clinicians*, vol. 71, pp. 209–249, 2021.

[2] I. Landa, T. Ibrahimpasic, L. Boucai et al., "Genomic and transcriptomic hallmarks of poorly differentiated and anaplastic thyroid cancers," *Journal of Clinical Investigation*, vol. 126, pp. 1052–1066, 2016.

[3] S. Filetti, C. Durante, D. Hartl et al., "Thyroid cancer: ESMO clinical practice guidelines for diagnosis, treatment and follow-up," *Annals of Oncology*, vol. 30, pp. 1856–1883, 2019.

[4] N. Pozdeyev, L. M. Gay, E. S. Sokol et al., "Genetic analysis of 779 advanced differentiated and anaplastic thyroid cancers," *Clinical Cancer Research*, vol. 24, pp. 3059–3068, 2018.

[5] B. J. Park, D. H. Lee, J. C. Park et al., "Sterilization using a microwave-induced argon plasma system at atmospheric pressure," *Physics of Plasmas*, vol. 10, pp. 4539–4544, 2003.

[6] D. H. Xu, Q. J. Cui, Y. J. Xu, D. X. Liu, and G. Y. Kong, "Plasma medicine and the application in tumor therapy," *Progress in Biochemistry and Biophysics*, vol. 44, pp. 279–292, 2017.

[7] G. Fridman, G. Friedman, A. Gutsol, A. B. Shekhter, V. N. Vasilets, and A. Fridman, "Applied plasma medicine," *Plasma Process and Polymers*, vol. 5, pp. 503–533, 2008.

[8] P. Bruggeman and C. Leys, "Non-thermal plasmas in and in contact with liquids," *Journal of Physics D Applied Physics*, vol. 42, Article ID 053001, 2009.

[9] Z. M. Xu, Y. Lan, J. Ma et al., "Applications of atmospheric pressure plasma in microbial inactivation and cancer therapy: a brief review," *Plasma Science and Technology*, vol. 22, Article ID 103001, 2020.

[10] Y. C. Yao, K. Song, H. Chen et al., "In vitro and in vivo research of atmosphere pressure nonequilibrium plasmas on root canal disinfection: implication for alternative strategy for irrigation," *Clinical Oral Investigations*, vol. 25, pp. 5833–5842, 2021.

[11] C. H. Song, P. Attri, S. K. Ku, I. Huan, A. Bogaerts, and E. H. Choi, "Cocktail of reactive species generated by cold atmospheric plasma: oral administration induces non-small cell lung cancer cell death," *Journal of Physics D Applied Physics*, vol. 54, Article ID 185202, 2021.

[12] G. Fridman, A. Shereshevsky, M. M. Jost et al., "Floating electrode dielectric barrier discharge plasma in air promoting apoptotic behavior in melanoma skin cancer cell lines," *Plasma Chemistry and Plasma Processing*, vol. 27, pp. 163–176, 2007.

[13] A. J. Kenari, S. N. Siadati, Z. Abedian et al., "Therapeutic effect of cold atmospheric plasma and its combination with radiation as a novel approach on inhibiting cervical cancer cell growth (HeLa cells)," *Bioorganic Chemistry*, vol. 111, Article ID 104892, 2021.

[14] S. U. Kang, S. J. Seo, Y. S. Kim et al., "Comparative effects of non-thermal atmospheric pressure plasma on migration and invasion in oral squamous cell cancer, by gas type," *Yonsei Medical Journal*, vol. 58, pp. 272–281, 2017.

[15] G. Uchida, T. Ito, J. Ikeda, T. Suzuki, K. Takenaka, and Y. Setsuhara, "Effect of a plasma-activated medium produced by direct irradiation on cancer cell killing," *Japanese Journal of Applied Physics*, vol. 57, Article ID 096201, 2018.

[16] S. Muneekaew, Y. H. Huang, and M. J. Wang, "Selective killing effects of atmospheric pressure plasma jet on human melanoma and lewis lung carcinoma cells," *Plasma Chemistry and Plasma Processing*, vol. 41, pp. 1613–1629, 2021.

[17] J. R. Liu, Y. M. Wu, G. M. Xu et al., "Low-temperature plasma induced melanoma apoptosis by triggering a p53/PIGs/caspase-dependent pathway in vivo and in vitro," *Journal of Physics D Applied Physics*, vol. 52, p. 31, 2019.

[18] J. Ma, H. Zhang, C. Cheng, J. Shen, L. Z. Bao, and W. Han, "Contribution of hydrogen peroxide to non-thermal atmospheric pressure plasma induced A549 lung cancer cell damage," *Plasma Processes and Polymers*, vol. 14, Article ID e1600162, 2017.

[19] S. B. Karki, T. T. Gupta, E. Y. Ayan, K. M. Eisenmann, and H. Ayan, "Miniature non-thermal plasma induced cell cycle arrest and apoptosis in lung carcinoma cells," *Plasma Chemistry and Plasma Processing*, vol. 40, p. 1, 2020.

[20] D. Yan, H. Xiao, W. Zhu et al., "The role of aquaporins in the anti-glioblastoma capacity of the cold plasma-stimulated

medium," *Journal of Physics D Applied Physics*, vol. 50, p. 5, 2017.

[21] M. Ishaq, K. Bazaka, and K. Ostrikov, "Pro-apoptotic NOXA is implicated in atmospheric-pressure plasma-induced melanoma cell death," *Journal of Physics D Applied Physics*, vol. 48, p. 46, 2015.

[22] T. Adachi, H. Tanaka, S. Nonomura et al., "Plasma-activated medium induces A549 cell injury via a spiral apoptotic cascade involving the mitochondrial-nuclear network," *Free Radical Biology and Medicine*, vol. 79, pp. 28–44, 2015.

[23] X. R. Yang, G. Chen, K. N. Yu et al., "Cold atmospheric plasma induces GSDME-dependent pyroptotic signaling pathway via ROS generation in tumor cells," *Cell Death & Disease*, vol. 11, p. 295, 2020.

[24] H. Zhang, J. S. Zhang, J. Ma et al., "Differential sensitivities of HeLa and MCF-7 cells at G1-, S-, G2-and M-phase of the cell cycle to cold atmospheric plasma," *Journal of Physics D: Applied Physics*, vol. 53, p. 12, 2020.

[25] S. B. Karki, T. T. Gupta, E. Y. Ayan, K. M. Eisenmann, and H. Ayan, "Investigation of non-thermal plasma effects on lung cancer cells within 3D collagen matrices," *Journal of Physics D Applied Physics*, vol. 50, p. 31, 2017.

[26] M. Akter, A. Jangra, S. A. Choi, E. H. Choi, and I. Han, "Non-thermal atmospheric pressure bio-compatible plasma stimulates apoptosis via p38/mapk mechanism in u87 malignant glioblastoma," *Cancers*, vol. 12, p. 245, 2020.

[27] J. W. Chang, S. U. Kang, Y. S. Shin et al., "Non-thermal atmospheric pressure plasma induces apoptosis in oral cavity squamous cell carcinoma: Involvement of DNA-damage-triggering sub-G (1) arrest via the ATM/p53 pathway," *Archives of Biochemistry and Biophysics*, vol. 545, pp. 133–140, 2014.

[28] S. Y. Lee, S. U. Kang, K. I. Kim et al., "Non-thermal plasma induces apoptosis in ATC cells: involvement of JNK and p38 MAPK-dependent ROS," *Yonsei Medical Journal*, vol. 55, pp. 1640–1647, 2014.

[29] J. W. Chang, S. U. Kang, Y. S. Shin et al., "Non-thermal atmospheric pressure plasma inhibits thyroid papillary cancer cell invasion via cytoskeletal modulation altered MMP-2/-9/ uPA Activity," *PLoS One*, vol. 9, Article ID e92198, 2014.

[30] H. Zhang, J. S. Zhang, S. D. Xu, D. X. Liu, L. Guo, and H. Li, "Study on the anticancer effects of a 7 mu m sized helium plasma jet on micro-tumors," *Journal of Physics D Applied Physics*, vol. 54, Article ID 385203, 2021.

[31] H. Zhang, J. S. Zhang, S. D. Xu et al., "Antitumor effects of hyperthermia with plasma-treated solutions on 3D bladder tumor spheroids," *Plasma Process and Polymer*, vol. 18, Article ID e2100070, 2021.

[32] A. Hadefi, M. Leprovots, M. Thulliez et al., "Cold atmospheric plasma differentially affects cell renewal and differentiation of stem cells and APC-deficient-derived tumor cells in intestinal organoids," *Cell Death Discovery*, vol. 8, p. 66, 2022.

[33] G. P. Melo, T. Nascimento, L. J. Sanches et al., "Plasma treatment limits cutaneous squamous cell carcinoma development in vitro and in vivo," *Cancers*, vol. 12, Article ID e, 2020.

[34] H. Zhang, J. Ma, J. Shen et al., "Comparison of the effects induced by plasma generated reactive species and H_2O_2 on lactate dehydrogenase (LDH) enzyme," *IEEE Transactions on Plasma Science*, vol. 46, pp. 2742–2752, 2018.

[35] C. A. Ferreira, R. S. Teixeira, M. Laranjo et al., "Open-air cold plasma device leads to selective tumor cell cytotoxicity," *Applied Sciences*, vol. 11, p. 4171, 2021.

[36] Y. Li, T. Tang, H. J. Lee, and K. Song, "Selective anti-cancer effects of plasma-activated medium and its high efficacy with cisplatin on hepatocellular carcinoma with cancer stem cell characteristics," *International Journal of Molecular Sciences*, vol. 22, p. 3956, 2021.

[37] Y. Li, T. Tang, H. J. Lee, and K. Song, "Cold atmospheric pressure plasma-activated medium induces selective cell death in human hepatocellular carcinoma cells independently of singlet oxygen, hydrogen peroxide, nitric oxide and nitrite/ nitrate," *International Journal of Molecular Sciences*, vol. 22, p. 5548, 2021.

[38] J. Tornin, M. Mateu-Sanz, A. Rodríguez, C. Labay, R. Rodriguez, and C. Canal, "Pyruvate plays a main role in the antitumoral selectivity of cold atmospheric plasma in osteosarcoma," *Scientific Reports*, vol. 9, Article ID 10681, 2019.

[39] G. Bauer, "Tumor cell-protective catalase as a novel target for rational therapeutic approaches based on specific intercellular ros signaling," *Anticancer Research*, vol. 32, pp. 2599–2624, 2012.

[40] J. Paal, S. H. Hong, M. Yusupov et al., "How membrane lipids influence plasma delivery of reactive oxygen species into cells and subsequent DNA damage: an experimental and computational study," *Physical Chemistry Chemical Physics*, vol. 21, Article ID 19327, 2019.

[41] S. Bekeschus, G. Liebelt, J. Menz et al., "Tumor cell metabolism correlates with resistance to gas plasma treatment: the evaluation of three dogmas," *Free Radical Biology and Medicine*, vol. 167, pp. 12–28, 2021.

[42] K. D. Weltmann, E. Kindel, T. V. Woedtke, M. Hahnel, M. Stieber, and R. Brandenburg, "Atmospheric-pressure plasma sources: prospective tools for plasma medicine," *Pure and Applied Chemistry*, vol. 82, pp. 1223–1237, 2010.

[43] U. Kogelschatz, "Dielectric-barrier discharges: their history, discharge physics, and industrial applications," *Plasma Chemistry and Plasma Processing*, vol. 23, pp. 1–46, 2003.

[44] H. Tanaka, S. Bekeschus, D. Yan, M. Hori, M. Keidar, and M. Laroussi, "Plasma-treated solutions (pts) in cancer therapy," *Cancers*, vol. 13, p. 1737, 2021.

[45] S. Hartwig, S. Preissner, J. O. Voss et al., "The feasibility of cold atmospheric plasma in the treatment of complicated wounds in cranio-maxillo-facial surgery," *Journal of Cranio-Maxillofacial Surgery*, vol. 45, pp. 1724–1730, 2017.

[46] M. M. Sanz, J. Tornín, B. Brulin et al., "Cold plasma-treated ringer's saline: a weapon to target osteosarcoma," *Cancers*, vol. 12, p. 227, 2020.

[47] W. Nupangtha, C. Kuensaen, S. Sarapirom, and D. Boonyawan, "Investigation of cold atmospheric plasma induce apoptosis in cancer cell," *Journal of Physics: Conference Series*, vol. 1144, Article ID 012025, 2018.

[48] P. Subramanian, A. Jain, A. M. Shivapuji, N. R. Sundaresan, S. Dasappa, and L. Rao, "Plasma-activated water from a dielectric barrier discharge plasma source for the selective treatment of cancer cells," *Plasma Process and Polymers*, vol. 17, Article ID e1900260, 2020.

[49] D. Yan, J. H. Sherman, and K. Michael, "Cold atmospheric plasma, a novel promising anti-cancer treatment modality," *Oncotarget*, vol. 8, Article ID 15977, 2017.

[50] Y. Y. Wang, C. Cheng, P. Gao et al., "Cold atmospheric-pressure air plasma treatment of c6 glioma cells: effects of reactive oxygen species in the medium produced by the plasma on cell death," *Plasma Science and Technology*, vol. 19, Article ID 025503, 2017.

[51] E. Gjika, S. Pal-Ghosh, A. Tang et al., "Adaptation of operational parameters of cold atmospheric plasma for in vitro

treatment of cancer cells," *Acs Applied Materials and Interfaces*, vol. 10, p. 9269, 2018.

[52] W. Martin, D. Gumbel, E. M. Hanschmann et al., "Cold atmospheric plasma treatment induces anti-proliferative effects in prostate cancer cells by redox and apoptotic signaling pathways," *PLoS One*, vol. 10, Article ID e0130350, 2015.

[53] J. K. Sun, H. M. Jon, and T. H. Chung, "Production of intracellular reactive oxygen species and change of cell viability induced by atmospheric pressure plasma in normal and cancer cells," *Applied Physics Letters*, vol. 103, p. R1, 2013.

[54] J. C. Guo, Z. Z. Yang, Y. Z. Lu et al., "An antioxidant system through conjugating superoxide dismutase onto metal-organic framework for cardiac repair," *Bioactive Materials*, vol. 10, pp. 56–67, 2022.

[55] H. R. Feng, X. Cheng, J. Kuang et al., "Apatinib-induced protective autophagy and apoptosis through the AKT-mTOR pathway in anaplastic thyroid cancer," *Cell Death & Disease*, vol. 9, p. 1030, 2018.

[56] K. Ohnishi, I. Ota, K. Yane et al., "Glycerol as a chemical chaperone enhances radiation-induced apoptosis in anaplastic thyroid carcinoma cells," *Molecular Cancer*, vol. 1, p. 4, 2002.

[57] S. L. Xu, Y. Wang, Y. K. Que et al., "Cold atmospheric plasma-activated ringer's solution inhibits the proliferation of osteosarcoma cells through the mitochondrial apoptosis pathway," *Oncology Reports*, vol. 43, pp. 1683–1691, 2020.

[58] J. Vaquero, F. Judee, M. Vallette et al., "Cold-atmospheric plasma induces tumor cell death in preclinical in vivo and in vitro models of human cholangiocarcinoma," *Cancers*, vol. 12, p. 1280, 2020.

[59] H. J. Ahn, K. I. Kim, N. N. Hoan et al., "Targeting cancer cells with reactive oxygen and nitrogen species generated by atmospheric-pressure air plasma," *PLoS One*, vol. 9, Article ID e86173, 2014.

[60] F. Xu, L. X. Na, Y. F. Li, and L. J. Chen, "Roles of the PI3K/AKT/mTOR signalling pathways in neurodegenerative diseases and tumours," *Cell and Bioscience*, vol. 10, p. 54, 2020.

[61] A. M. G. Angulo and G. R. Blumenschein, "Defining biomarkers to predict sensitivity to PI3K/Akt/mTOR pathway inhibitors in breast cancer," *Cancer Treatment Reviews*, vol. 39, pp. 313–320, 2013.

[62] Y. L. Cai, X. D. Tan, J. Liu et al., "Inhibition of PI3K/Akt/mTOR signaling pathway enhances the sensitivity of the SKOV3/DDP ovarian cancer cell line," *Chinese Journal of Cancer Research*, vol. 26, pp. 564–572, 2014.

[63] M. H. Ung, G. L. Wang, F. S. Varn, and C. Chen, "Application of pharmacologically induced transcriptomic profiles to interrogate PI3K-Akt-mTOR pathway activity associated with cancer patient prognosis," *Oncotarget*, vol. 7, Article ID 84142, 2016.

[64] C. X. Guo, M. Yang, L. Jing et al., "Amorphous silica nanoparticles trigger vascular endothelial cell injury through apoptosis and autophagy via reactive oxygen species-mediated MAPK/Bcl-2 and PI3K/Akt/mTOR signaling," *International Journal of Nanomedicine*, vol. 11, pp. 5257–5276, 2016.

[65] E. Griseti, N Merbahi, and M. Golzio, "Anti-cancer potential of two plasma-activated liquids: implication of long-lived reactive oxygen and nitrogen species," *Cancers*, vol. 12, p. 721, 2020.

[66] S. H. Yang, T. Zhao, L. Zou, X. L. Wang, and Y. T. Zhang, "ReaxFF-based molecular dynamics simulation of DNA molecules destruction in cancer cells by plasma ROS," *Physics of Plasmas*, vol. 26, Article ID 083504, 2019.

[67] D. Xu, Q. J. Cui, Y. J. Xu et al., "and $NO_3^- NO_2^-$ enhance cold atmospheric plasma induced cancer cell death by generation of $ONOO^-$," *AIP Advances*, vol. 8, Article ID 105219, 2018.

[68] J. H. Lee, J. Y. Om, Y. H. Kim, K. M. Kim, E. H. Choi, and K. N. Kim, "Selective killing effects of cold atmospheric pressure plasma with no induced dysfunction of epidermal growth factor receptor in oral squamous cell carcinoma," *PLoS One*, vol. 11, 2016 https://doi.org/10.1371/journal.pone.0150279, Article ID e0150279.

[69] G. Bauer, "The synergistic effect between hydrogen peroxide and nitrite, two long-lived molecular species from cold atmospheric plasma, triggers tumor cells to induce their own cell death," *Redox Biology*, vol. 26, Article ID 101291, 2019.